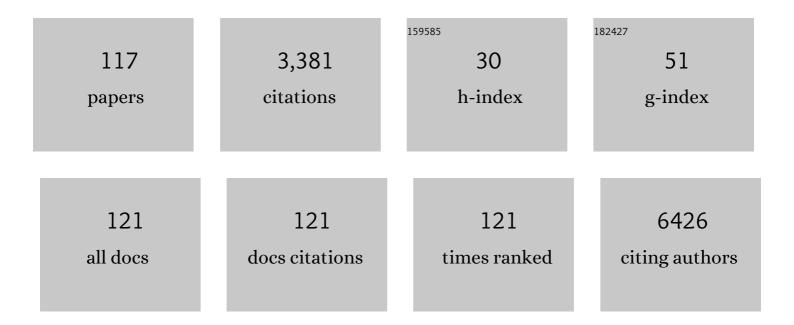
List of Publications by Year in descending order

Source: https://exaly.com/author-pdf/6097484/publications.pdf Version: 2024-02-01



KENNETH LIONES

#	Article	IF	CITATIONS
1	Germline mutations in ETV6 are associated with thrombocytopenia, red cell macrocytosis and predisposition to lymphoblastic leukemia. Nature Genetics, 2015, 47, 535-538.	21.4	274
2	High-efficiency reprogramming of fibroblasts into cardiomyocytes requires suppression of pro-fibrotic signalling. Nature Communications, 2015, 6, 8243.	12.8	197
3	Islet-Derived CD4 T Cells Targeting Proinsulin in Human Autoimmune Diabetes. Diabetes, 2017, 66, 722-734.	0.6	154
4	Autophagy Supports Breast Cancer Stem Cell Maintenance by Regulating IL6 Secretion. Molecular Cancer Research, 2015, 13, 651-658.	3.4	152
5	Filamin C Truncation Mutations Are Associated With Arrhythmogenic DilatedÂCardiomyopathy and Changes inÂthe Cell–Cell Adhesion Structures. JACC: Clinical Electrophysiology, 2018, 4, 504-514.	3.2	125
6	Single-Cell Transcriptomic Analyses of the Developing Meninges Reveal Meningeal Fibroblast Diversity and Function. Developmental Cell, 2020, 54, 43-59.e4.	7.0	122
7	High-efficiency RNA-based reprogramming of human primary fibroblasts. Nature Communications, 2018, 9, 745.	12.8	117
8	Characterization of the resistome in manure, soil and wastewater from dairy and beef production systems. Scientific Reports, 2016, 6, 24645.	3.3	112
9	Novel insights into the clinical phenotype and pathophysiology underlying low VWF levels. Blood, 2017, 130, 2344-2353.	1.4	98
10	Genomewide Association Study of African Children Identifies Association of SCHIP1 and PDE8A with Facial Size and Shape. PLoS Genetics, 2016, 12, e1006174.	3.5	81
11	Enrichment allows identification of diverse, rare elements in metagenomic resistome-virulome sequencing. Microbiome, 2017, 5, 142.	11.1	78
12	MLL2, Not MLL1, Plays a Major Role in Sustaining MLL-Rearranged Acute Myeloid Leukemia. Cancer Cell, 2017, 31, 755-770.e6.	16.8	72
13	Role of Titin Missense Variants in Dilated Cardiomyopathy. Journal of the American Heart Association, 2015, 4, .	3.7	64
14	The molecular anatomy of mammalian upper lip and primary palate fusion at single cell resolution. Development (Cambridge), 2019, 146, .	2.5	63
15	Comparison of Varicella-Zoster Virus RNA Sequences in Human Neurons and Fibroblasts. Journal of Virology, 2014, 88, 5877-5880.	3.4	62
16	The FaceBase Consortium: A comprehensive resource for craniofacial researchers. Development (Cambridge), 2016, 143, 2677-88.	2.5	62
17	Impaired mitophagy facilitates mitochondrial damage in Danon disease. Journal of Molecular and Cellular Cardiology, 2017, 108, 86-94.	1.9	57
18	Systems biology of facial development: contributions of ectoderm and mesenchyme. Developmental Biology, 2017, 426, 97-114.	2.0	49

#	Article	IF	CITATIONS
19	Gamma Interferon Alters Junctional Integrity via Rho Kinase, Resulting in Blood-Brain Barrier Leakage in Experimental Viral Encephalitis. MBio, 2019, 10, .	4.1	48
20	Autoimmune vitiligo is associated with gain-of-function by a transcriptional regulator that elevates expression of <i>HLA-A*02:01</i> in vivo. Proceedings of the National Academy of Sciences of the United States of America, 2016, 113, 1357-1362.	7.1	46
21	Development of new preclinical models to advance adrenocortical carcinoma research. Endocrine-Related Cancer, 2018, 25, 437-451.	3.1	45
22	Specific expression of PDâ€L1 in RELAâ€fusion supratentorial ependymoma: Implications for PDâ€1â€ŧargeted therapy. Pediatric Blood and Cancer, 2018, 65, e26960.	1.5	44
23	Replication of High Fetal Alcohol Spectrum Disorders Prevalence Rates, Child Characteristics, and Maternal Risk Factors in a Second Sample of Rural Communities in South Africa. International Journal of Environmental Research and Public Health, 2017, 14, 522.	2.6	43
24	Joint MiRNA/mRNA Expression Profiling Reveals Changes Consistent with Development of Dysfunctional Corpus Luteum after Weight Gain. PLoS ONE, 2015, 10, e0135163.	2.5	42
25	Senescence Induced by BMI1 Inhibition Is a Therapeutic Vulnerability in H3K27M-Mutant DIPG. Cell Reports, 2020, 33, 108286.	6.4	39
26	AP-2α and AP-2β cooperatively orchestrate homeobox gene expression during branchial arch patterning. Development (Cambridge), 2018, 145, .	2.5	35
27	PERSPECTIVES ON THE CAUSE AND FREQUENCY OF THE FETAL ALCOHOL SYNDROME. Annals of the New York Academy of Sciences, 1976, 273, 138-139.	3.8	34
28	Combined Face–Brain Morphology and Associated Neurocognitive Correlates in Fetal Alcohol Spectrum Disorders. Alcoholism: Clinical and Experimental Research, 2018, 42, 1769-1782.	2.4	34
29	The Jumonji-domain histone demethylase inhibitor JIB-04 deregulates oncogenic programs and increases DNA damage in Ewing Sarcoma, resulting in impaired cell proliferation and survival, and reduced tumor growth. Oncotarget, 2018, 9, 33110-33123.	1.8	34
30	Single Cell RNA Sequencing of Human Milk-Derived Cells Reveals Sub-Populations of Mammary Epithelial Cells with Molecular Signatures of Progenitor and Mature States: a Novel, Non-invasive Framework for Investigating Human Lactation Physiology. Journal of Mammary Gland Biology and Neoplasia, 2020, 25, 367-387.	2.7	33
31	NF-κB upregulation through epigenetic silencing of LDOC1 drives tumor biology and specific immunophenotype in Group A ependymoma. Neuro-Oncology, 2017, 19, 1350-1360.	1.2	32
32	Increased galactose expression and enhanced clearance in patients with low von Willebrand factor. Blood, 2019, 133, 1585-1596.	1.4	32
33	Comprehensive molecular characterization of pediatric radiation-induced high-grade glioma. Nature Communications, 2021, 12, 5531.	12.8	31
34	Facial Curvature Detects and Explicates Ethnic Differences in Effects of Prenatal Alcohol Exposure. Alcoholism: Clinical and Experimental Research, 2017, 41, 1471-1483.	2.4	28
35	Nitric Oxide from IFNÎ ³ -Primed Macrophages Modulates the Antimicrobial Activity of Î ² -Lactams against the Intracellular Pathogens Burkholderia pseudomallei and Nontyphoidal Salmonella. PLoS Neglected Tropical Diseases, 2014, 8, e3079.	3.0	25
36	FaceBase 3: analytical tools and FAIR resources for craniofacial and dental research. Development (Cambridge), 2020, 147, .	2.5	25

#	Article	IF	CITATIONS
37	Genome Replication in Thermococcus kodakarensis Independent of Cdc6 and an Origin of Replication. Frontiers in Microbiology, 2017, 8, 2084.	3.5	24
38	Activity of Combined Androgen Receptor Antagonism and Cell Cycle Inhibition in Androgen Receptor Positive Triple Negative Breast Cancer. Molecular Cancer Therapeutics, 2021, 20, 1062-1071.	4.1	24
39	Onset of taste bud cell renewal starts at birth and coincides with a shift in SHH function. ELife, 2021, 10, .	6.0	24
40	Genomic single-nucleotide polymorphisms confirm that Gunnison and Greater sage-grouse are genetically well differentiated and that the Bi-State population is distinct. Condor, 2015, 117, 217-227.	1.6	20
41	Increased FGF8 signaling promotes chondrogenic rather than osteogenic development in the embryonic skull. DMM Disease Models and Mechanisms, 2018, 11, .	2.4	20
42	PARP Inhibition Enhances Radiotherapy of SMAD4-Deficient Human Head and Neck Squamous Cell Carcinomas in Experimental Models. Clinical Cancer Research, 2020, 26, 3058-3070.	7.0	20
43	An autonomous metabolic role for Spen. PLoS Genetics, 2017, 13, e1006859.	3.5	19
44	Idiopathic Scoliosis Families Highlight Actin-Based and Microtubule-Based Cellular Projections and Extracellular Matrix in Disease Etiology. G3: Genes, Genomes, Genetics, 2018, 8, 2663-2672.	1.8	19
45	Transcriptional profiling of murine retinas undergoing semi-synchronous cone photoreceptor differentiation. Developmental Biology, 2019, 453, 155-167.	2.0	19
46	Robust deep learning classification of adamantinomatous craniopharyngioma from limited preoperative radiographic images. Scientific Reports, 2020, 10, 16885.	3.3	19
47	Combined ASBT Inhibitor and FGF15 Treatment Improves Therapeutic Efficacy in Experimental Nonalcoholic Steatohepatitis. Cellular and Molecular Gastroenterology and Hepatology, 2021, 12, 1001-1019.	4.5	19
48	Compromised global embryonic transcriptome associated with advanced maternal age. Journal of Assisted Reproduction and Genetics, 2019, 36, 915-924.	2.5	18
49	Development and characterization of twenty-two novel microsatellite markers for the mountain whitefish, Prosopium williamsoni and cross-amplification in the round whitefish, P. cylindraceum, using paired-end Illumina shotgun sequencing. Conservation Genetics Resources, 2013, 5, 89-91.	0.8	17
50	High resolution measurement of DUF1220 domain copy number from whole genome sequence data. BMC Genomics, 2017, 18, 614.	2.8	17
51	FGF signaling directs myotube guidance by regulating Rac activity. Development (Cambridge), 2020, 147,	2.5	17
52	Mutations in <i>KIF7</i> implicated in idiopathic scoliosis in humans and axial curvatures in zebrafish. Human Mutation, 2021, 42, 392-407.	2.5	17
53	AP-2α and AP-2β cooperatively function in the craniofacial surface ectoderm to regulate chromatin and gene expression dynamics during facial development. ELife, 2022, 11, .	6.0	17
54	Development and characterization of sixteen microsatellite markers for the federally endangered species: Leptodea leptodon (Bivalvia: Unionidae) using paired-end Illumina shotgun sequencing. Conservation Genetics Resources, 2012, 4, 787-789.	0.8	16

#	Article	IF	CITATIONS
55	MEMO1 drives cranial endochondral ossification and palatogenesis. Developmental Biology, 2016, 415, 278-295.	2.0	16
56	Detection of pro angiogenic and inflammatory biomarkers in patients with CKD. Scientific Reports, 2021, 11, 8786.	3.3	16
57	Initiation of <i>Otx2</i> expression in the developing mouse retina requires a unique enhancer and either <i>Ascl1</i> or <i>Neurog2</i> activity. Development (Cambridge), 2021, 148, .	2.5	16
58	Deficiency of mitochondrial modulator MCJ promotes chemoresistance in breast cancer. JCI Insight, 2016, 1, .	5.0	16
59	The Elovl4 Spinocerebellar Ataxia-34 Mutation 736T>G (p.W246G) Impairs Retinal Function in the Absence of Photoreceptor Degeneration. Molecular Neurobiology, 2020, 57, 4735-4753.	4.0	15
60	ETV6 germline mutations cause HDAC3/NCOR2 mislocalization and upregulation of interferon response genes. JCI Insight, 2020, 5, .	5.0	15
61	<i>Csg1</i> , <i>Trnp1</i> , and <i>Tmem215</i> Mark Subpopulations of Bipolar Interneurons in the Mouse Retina. , 2017, 58, 1137.		14
62	Increased HDAC Activity and c-MYC Expression Mediate Acquired Resistance to WEE1 Inhibition in Acute Leukemia. Frontiers in Oncology, 2020, 10, 296.	2.8	14
63	Breast Cancer Endocrine Therapy Promotes Weight Gain With Distinct Adipose Tissue Effects in Lean and Obese Female Mice. Endocrinology, 2021, 162, .	2.8	14
64	Histamine H2 Receptor Polymorphisms, Myocardial Transcripts, and Heart Failure (from the) Tj ETQq0 0 0 rgBT	/Overlock 1.6	10 Tf 50 387 1 13
65	Distinct pathways affected by menin versus MLL1/MLL2 in MLL-rearranged acute myeloid leukemia. Experimental Hematology, 2019, 69, 37-42.	0.4	13
66	Hypertonic saline attenuates the cytokine-induced pro-inflammatory signature in primary human lung epithelia. PLoS ONE, 2017, 12, e0189536.	2.5	13
67	PRDM paralogs antagonistically balance Wnt/β-catenin activity during craniofacial chondrocyte differentiation. Development (Cambridge), 2022, 149, .	2.5	13
68	Occupancy of RNA Polymerase II Phosphorylated on Serine 5 (RNAP S5 ^P) and RNAP S2 ^P on Varicella-Zoster Virus Genes 9, 51, and 66 Is Independent of Transcript Abundance and Polymerase Location within the Gene. Journal of Virology, 2016, 90, 1231-1243.	3.4	12
69	An Alternative Splicing Program for Mouse Craniofacial Development. Frontiers in Physiology, 2020, 11, 1099.	2.8	12
70	Hypertonic Saline Primes Activation of the p53–p21 Signaling Axis in Human Small Airway Epithelial Cells That Prevents Inflammation Induced by Pro-inflammatory Cytokines. Journal of Proteome Research, 2016, 15, 3813-3826.	3.7	11
71	Establishment of patient-derived orthotopic xenograft model of 1q+ posterior fossa group A ependymoma. Neuro-Oncology, 2019, 21, 1540-1551.	1.2	11
72	Calorie restriction prevents age-related changes in the intestinal microbiota. Aging, 2021, 13, 6298-6329.	3.1	11

#	Article	IF	CITATIONS
73	KDM3A/Ets1/MCAM axis promotes growth and metastatic properties in Rhabdomyosarcoma. Genes and Cancer, 2020, 11, 53-65.	1.9	11
74	Transient Expression of GATA3 in Hematopoietic Stem Cells Facilitates Helper Innate Lymphoid Cell Differentiation. Frontiers in Immunology, 2019, 10, 510.	4.8	10
75	Human innate lymphoid cell precursors express CD48 that modulates ILC differentiation through 2B4 signaling. Science Immunology, 2020, 5, .	11.9	10
76	Development and characterization of twenty-three microsatellite markers for the freshwater minnow Santa Ana speckled dace (Rhinichthys osculus spp., Cyprinidae) using paired-end Illumina shotgun sequencing. Conservation Genetics Resources, 2013, 5, 145-148.	0.8	9
77	Targeted Genome Sequencing Reveals Varicella-Zoster Virus Open Reading Frame 12 Deletion. Journal of Virology, 2017, 91, .	3.4	9
78	Whole Exome Sequencing of 23 Multigeneration Idiopathic Scoliosis Families Reveals Enrichments in Cytoskeletal Variants, Suggests Highly Polygenic Disease. Genes, 2021, 12, 922.	2.4	9
79	Combined deletion of Xrcc4 and Trp53 in mouse germinal center B cells leads to novel B cell lymphomas with clonal heterogeneity. Journal of Hematology and Oncology, 2016, 9, 2.	17.0	8
80	Investigation of Islet2a function in zebrafish embryos: Mutants and morphants differ in morphologic phenotypes and gene expression. PLoS ONE, 2018, 13, e0199233.	2.5	8
81	Sequential analysis of myocardial gene expression with phenotypic change: Use of cross-platform concordance to strengthen biologic relevance. PLoS ONE, 2019, 14, e0221519.	2.5	8
82	Proteasome inhibition as a therapeutic approach in atypical teratoid/rhabdoid tumors. Neuro-Oncology Advances, 2020, 2, vdaa051.	0.7	8
83	Prolactin Acts on Myeloid Progenitors to Modulate SMAD7 Expression and Enhance Hematopoietic Stem Cell Differentiation into the NK Cell Lineage. Scientific Reports, 2020, 10, 6335.	3.3	8
84	MLL1 Promotes IL-7 Responsiveness and Survival during B Cell Differentiation. Journal of Immunology, 2018, 200, 1682-1691.	0.8	7
85	KDM5A and PHF2 positively control expression of pro-metastatic genes repressed by EWS/Fli1, and promote growth and metastatic properties in Ewing sarcoma. Oncotarget, 2020, 11, 3818-3831.	1.8	7
86	Physical Forces in Glioblastoma Migration: A Systematic Review. International Journal of Molecular Sciences, 2022, 23, 4055.	4.1	7
87	Development and characterization of thirty novel microsatellite markers for the critically endangered Myanmar Roofed Turtle, Batagur trivittata, and cross-amplification in the Painted River Terrapin, B. borneoensis, and the Southern River Terrapin, B. affinis, using paired-end Illumina shotgun sequencing. Conservation Genetics Resources. 2013. 5, 383-387.	0.8	6
88	Development and characterization of twenty-two polymorphic microsatellite markers for the leafcutter ant, Acromyrmex lundii, utilizing Illumina sequencing. Conservation Genetics Resources, 2014, 6, 319-322.	0.8	6
89	Development of microsatellite markers for buffalograss (Buchloë dactyloides ; Poaceae), a droughtâ€ŧolerant turfgrass alternative. Applications in Plant Sciences, 2016, 4, 1600033.	2.1	6
90	A method for extracting and characterizing RNA from urine: For downstream PCR and RNAseq analysis. Analytical Biochemistry, 2017, 536, 8-15.	2.4	6

#	ARTICLE	IF	CITATIONS
91	Development of 28 polymorphic microsatellite markers for the endemic Azorean spider Sancus acoreensis (Araneae, Tetragnathidae). Conservation Genetics Resources, 2013, 5, 1133-1134.	0.8	5
92	Characterization of microsatellite loci for an Australian epiphytic orchid, Dendrobium calamiforme , using Illumina sequencing. Applications in Plant Sciences, 2015, 3, 1500016.	2.1	5
93	In vivo interferon-gamma induced changes in gene expression dramatically alter neutrophil phenotype. PLoS ONE, 2022, 17, e0263370.	2.5	5
94	Fourteen novel microsatellite markers for the gopher frog, Lithobates capito (Amphibia: Ranidae). Conservation Genetics Resources, 2012, 4, 201-203.	0.8	4
95	Development of polymorphic microsatellite markers for the microendemic pupfishes Cyprinodon julimes and C. pachycephalus. Conservation Genetics Resources, 2013, 5, 853-856.	0.8	4
96	Twelve novel microsatellite markers for the marbled salamander, Ambystoma opacum. Conservation Genetics Resources, 2011, 3, 773-775.	0.8	3
97	Development of polymorphic microsatellite markers for blue king crab (Paralithodes platypus). Conservation Genetics Resources, 2012, 4, 897-899.	0.8	3
98	Development of 31 polymorphic microsatellite markers for the mole salamander (Ambystoma) Tj ETQq0 0 0 rgB1	- /Overlock	19 Tf 50 46
99	Isolation and characterization of 18 novel polymorphic microsatellite markers from the Mayan cichlid (Cichlasoma urophthalmus). Conservation Genetics Resources, 2013, 5, 703-705.	0.8	3
100	Development of twenty-one polymorphic microsatellite markers for the fungus-growing ant, Mycocepurus goeldii (Formicidae: Attini), using Illumina paired-end genomic sequencing. Conservation Genetics Resources, 2014, 6, 739-741.	0.8	3
101	Development of polymorphic microsatellite markers for the North American porcupine, Erethizon dorsatum, using paired-end Illumina sequencing. Conservation Genetics Resources, 2013, 5, 925-927.	0.8	2
102	Development of polymorphic microsatellite markers for the Pleuroderma thaul. Conservation Genetics Resources, 2014, 6, 747-749.	0.8	2
103	Development and characterization of 33 novel polymorphic microsatellite markers for the brown tree snake Boiga irregularis. BMC Research Notes, 2015, 8, 658.	1.4	2
104	Development of polymorphic microsatellite markers for the bonnethead shark, Sphyrna tiburo. Conservation Genetics Resources, 2015, 7, 69-71.	0.8	2
105	Unexpected effects of different genetic backgrounds on identification of genomic rearrangements via whole-genome next generation sequencing. BMC Genomics, 2016, 17, 823.	2.8	2
106	Enrichment of ovine gonadotropes via adenovirus gene targeting enhances assessment of transcriptional changes in response to estradiol-17 betaâ€. Biology of Reproduction, 2020, 102, 156-169.	2.7	2
107	Development and characterization of genomic resources for a non-model marine teleost, the red snapper (Lutjanus campechanus, Lutjanidae): Construction of a high-density linkage map, anchoring of genome contigs and comparative genomic analysis. PLoS ONE, 2020, 15, e0232402.	2.5	2
108	Single-Cell RNA-Seq Analysis of Native Murine Megakaryocytes from Young and Old Mice Reveals Significant Metabolic and Mitochondrial Differences throughout Megakaryocyte Development. Blood, 2018, 132, 1286-1286.	1.4	2

#	Article	IF	CITATIONS
109	Development and characterization of thirty-three microsatellite markers for the Patagonian sprat, Sprattus fuegensis (Jenyns, 1842), using paired-end Illumina shotgun sequencing. Conservation Genetics Resources, 2014, 6, 833-836.	0.8	1
110	Development of polymorphic microsatellite markers for the orange-breasted falcon (Falco) Tj ETQq0 0 0 rgBT /Ove	erlogk 10 T	f 50 702 To
111	Development and characterization of 30 novel microsatellite markers for Grant's gazelle (Nanger) Tj ETQq1 1	0,784314 0.8	rgBT /Overl
112	DIPC-66. THE H3K27M MUTATION CAUSES WIDE-RANGING CHANGES MEDIATING DIPG TUMORIGENESIS. Neuro-Oncology, 2018, 20, i62-i62.	1.2	0
113	II-08â€Complement receptors 1 and 2 on B cell subsets are negatively associated with lupus disease activity. , 2018, , .		0
114	HGG-45. COMPREHENSIVE MOLECULAR CHARACTERIZATION OF PEDIATRIC TREATMENT-INDUCED HIGH-GRADE GLIOMA: GERMLINE DNA REPAIR DEFECTS AS A POTENTIAL ETIOLOGY. Neuro-Oncology, 2018, 20, i98-i98.	1.2	0
115	Differential DNA Methylation of Human Metastable Epialleles in Guatemalan Infants at Birth Due to Timing of a Maternal Lipid-Based Nutrition Supplement and Pre-Pregnancy BMI (P11-139-19). Current Developments in Nutrition, 2019, 3, nzz048.P11-139-19.	0.3	0
116	Liver X Receptor (LXR) Is a Novel and Reversible Regulator of Trauma-Induced Coagulopathy. Blood, 2020, 136, 2-2.	1.4	0
117	Role of a Preconception Maternal Nutrition Supplement and Pre-pregnancy BMI on Amnion DNA Methylation at Birth in Guatemalan Mother-Infant Dyads: The Women First Trial. Current Developments in Nutrition, 2022, 6, 625	0.3	0